ELSEVIER

Journal of Alloys and Compounds 317–318 (2001) 222–226

Journal of ALLOYS AND COMPOUNDS

www.elsevier.com/locate/jallcom

# In-plane anisotropy of the optical and electrical properties of $ReS_2$ and $ReSe_2$ layered crystals

C.H. Ho[a,*], Y.S. Huang[b], K.K. Tiong[c]

[a]*Department of Electronic Engineering, Kuang Wu Institute of Technology, Peitou, Taipei 112, Taiwan, ROC*
[b]*Department of Electronic Engineering, National Taiwan University of Science and Technology, Taipei 106, Taiwan, ROC*
[c]*Department of Electrical Engineering, National Taiwan Ocean University, Keelung 202, Taiwan, ROC*

**Abstract**

$ReS_2$ and $ReSe_2$ belong to the family of transition-metal dichalcogenides crystallized in the distorted octahedral layer structure of triclinic symmetry. Crystals with triclinic symmetry are optically biaxial. The interband transitions of $ReS_2$ and $ReSe_2$ are expected to show anisotropic character for linearly polarized light, incident normal to the basal plane. The optical anisotropic effects for $E \| b$ and $E \perp b$ polarizations were studied through polarization-dependent piezoreflectance (PzR) and optical absorption measurements. The polarization dependence of the PzR spectra provides conclusive evidence that the features associated with the interband excitonic transitions are originated from different origins. The results of absorption measurements indicate that $ReS_2$ and $ReSe_2$ are indirect semiconductors, in which $E$ parallel to $b$-axis polarization exhibits a smaller band gap and a single phonon makes an important contribution in assisting the indirect transitions. The electrical conductivity along the $b$-axis was shown to be several times higher than that perpendicular to b-axis for both crystals. 

*Keywords:* Transition-metal dichalcogenides; Anisotropy; Optical property; Electrical property

## 1. Introduction

Layered $ReS_2$ and $ReSe_2$ are diamagnetic semiconductors and belong to the family of the transition-metal dichalcogenides [1,2]. The properties of the transition-metal dichalcogenides have been reviewed by Wilson and Yoffe [1]. The layered-type transition-metal dichalcogenides crystallized in a lattice with strong intralayer covalent bonds and weak interlayer interactions, usually of the van der Waals type. The strong anisotropy in the chemical bonds leads to anisotropy in many material properties parallel and perpendicular to the layers [3]. Unlike most of the layered transition-metal dichalcogenides, $ReX_2$ (X=S, Se) exhibits a distorted $CdCl_2$ structure, leading to triclinic symmetry [2,4,5]. Crystals with triclinic symmetry are optically biaxial. Therefore, anisotropic response of $ReX_2$ is expected for linearly polarized light, incident normal to the basal plane [$E \| (001)$, $k \perp (001)$]. This behavior differs from that of layered transition-metal dichalcogenides with hexagonal structure (e.g. 2 H–$MoS_2$ and $MoSe_2$), which are optically uniaxial with the optical axis perpendicular to the van der Waals plane. Wilson and Yoffe claimed biaxial behavior in the triclinic $ReS_2$. Friemelt et al. [6] in a recent article, reported anisotropic effects in the van der Waals plane of $ReS_2$ single crystals and suggested $ReS_2$ as a potential candidate for fabrication of polarization sensitive photodetectors in the visible wavelength region. However, to date, no detailed anisotropic optical and electrical properties for both $ReS_2$ and $ReSe_2$ in the van der Waals plane have been reported.

In this paper, a systematic study of the anisotropic optical and electrical properties of $ReS_2$ and $ReSe_2$ single crystals in the van der Waals plane is presented. The in-plane anisotropy of the direct band-edge excitons and indirect band-edge absorption are respectively studied at 25 and 300 K by polarization dependent piezoreflectance (PzR) and transmittance. In addition, the anisotropic effects of the carrier transport property are studied by the temperature dependent conductivity measurements along and perpendicular to the $b$-axis in the temperature range from 80 to 300 K. The results indicate a much larger electrical conductivity along the $b$-axis than that perpendicular to the $b$-axis.

*Corresponding author.
*E-mail address:* chhwho@ms28.hinet.net (C.H. Ho).

0925-8388/01/$ – see front matter 
PII: S0925-8388(00)01332-3

## 2. Experimental details

Single crystals of $ReS_2$ and $ReSe_2$ were grown using the chemical vapor transport method with $Br_2$ as the transport agent. Prior to the crystal growth, quartz tubes containing bromine and the elements (Re: 99.95% pure, S: 99.999%, Se: 99.999%) were evacuated and sealed. To improve the stoichiometry, sulfur or selenium with 2 mol% in excess was added with respect to rhenium. The quartz tube was placed in a three-zone furnace and the charge prereacted for 24 h at 800°C while the temperature of the growth zone was set at 1000°C to prevent the transport of the product. The furnace was then equilibrated to give a constant temperature across the reaction tube, and was programmed over 24 h to produce the temperature gradient at which single crystal growth takes place. Best results were obtained with temperature gradients of about 1060→1010°C for $ReS_2$ and 1050→1000°C for $ReSe_2$. After approximately 480 h, both $ReS_2$ and $ReSe_2$ single crystals formed thin, silver-colored, graphite-like, hexagonal platelets up to 2 $cm^2$ in area and 100 μm in thickness. X-ray diffraction patterns of single crystals confirmed the triclinic symmetry of $ReS_2$ and $ReSe_2$ with all parameters consistent with those previously reported [2,5,7]. Electron probe microanalysis indicated a chalcogen deficiency of approximately one percent in the crystals. Hall measurements revealed n-type semiconducting behavior. The weak van der Waals bonding between individual layers of the crystals means that they display good cleavage properties parallel to the layers and which can be exploited to obtain thin specimens.

Measurements of the reflectance and transmittance at near-normal incidence were made in the range 8000–13 500 $cm^{-1}$, with a resolution of 4 $cm^{-1}$. Transmission intensity was closely monitored to obtain an incidence as close to 90° as possible. Single crystals with a thickness of about 10 μm were used for transmittance measurements. Plate-shaped crystals were selected and mounted on a copper sample holder fitted into a Dewar with optical windows. The PzR measurements were achieved by gluing the thin single crystal specimens on a 0.15 cm thick lead-zirconate-titanate (PZT) piezoelectric transducer driven by a 200 $V_{rms}$ sinusoidal wave at 200 Hz. A 150 W tungsten-halogen lamp filtered by a 0.35 m monochromator which provided the monochromatic light. The reflected light was detected by a silicon photodiode, and the signal was recorded from a lock-in amplifier. A closed-cycle cryogenic refrigerator equipped with a digital thermometer controller was used for low temperature measurements. A near infrared dichroic sheet polarizers were employed for polarization dependent measurements.

The temperature dependence of conductivity was studied between 80 and 300 K by using a four-probe potentiometric technique. The selected sample was cut into a rectangular shape. Electrical connections to the crystal were made by means of four parallel gold wires (parallel or perpendicular to *b*-axis) laid across the basal surface of the thin crystal and attached to the crystal surface by means of conducting silver paint. The wires near each end of the rectangular crystal acted as current leads while the two contact wires on either side of the central line were used to measure the potential difference *V* in the crystal. The potential difference *V* measured by a sensitive potentiometer is the average value obtained on reversing the current through the sample. The crystal morphology and the crystal structure in the van der Waals plane of $ReS_2$ are shown in Fig. 1. The as-grown thin dark line in the crystal plane corresponds to the orientation of the *b*-axis. The *b*- and *a*-axes are the shortest and second shortest axes in the basal plane; the *b*-axis is parallel to the Re-cluster chains, which corresponds to the longest edge of the plate.

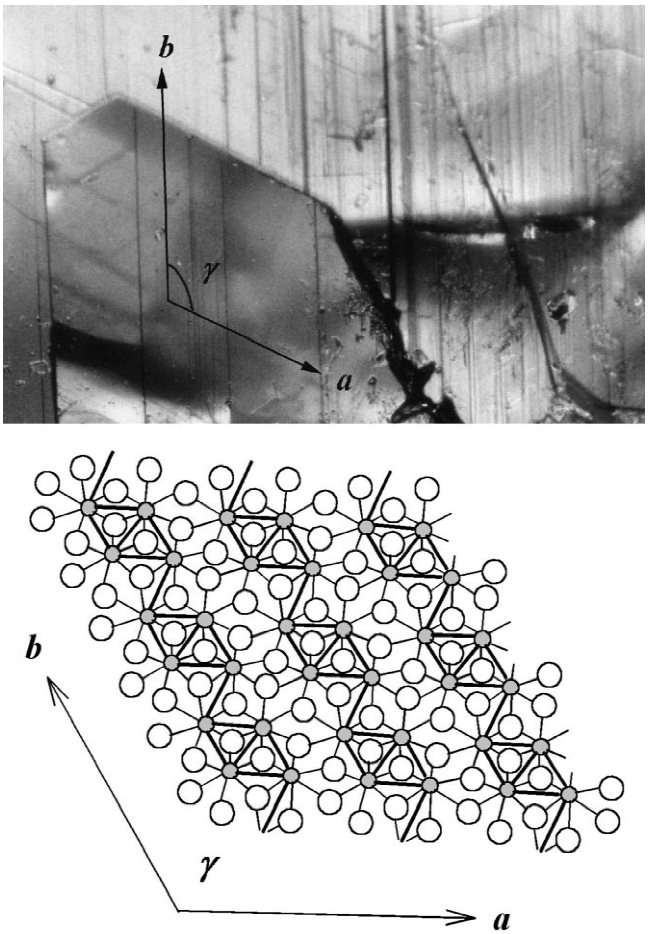


Fig. 1. The crystal morphology and crystal structure in the van der Waals plane of $ReS_2$ single crystals. The as-grown thin dark lines in the crystal plane corresponds to the orientation of *b*-axis.

## 3. Results and discussion

The polarization dependent PzR spectra of $ReS_2$ and $ReSe_2$ in the vicinity of the direct gap at 25 and 300 K are shown in Fig. 2a and b, respectively. The dashed curves

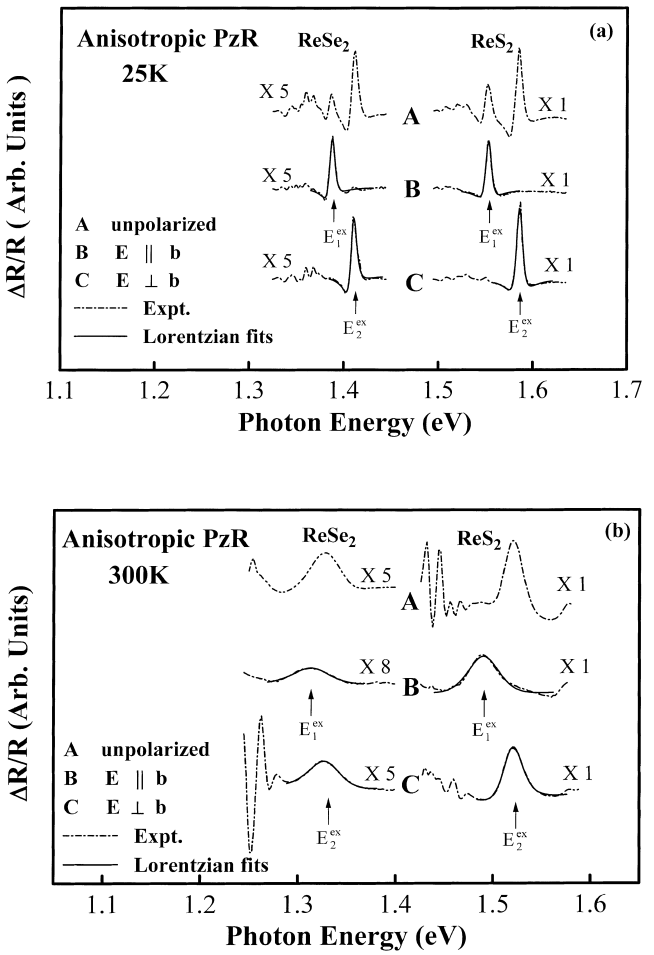


Fig. 2. The polarization dependent PzR spectra (dashed curves) of $ReS_2$ and $ReSe_2$ at (a) 25 K and (b) 300 K. The solid lines are least-squares fits to the Lorentzian line-shape form which yields the excitonic transition energies indicated by arrows.

are the experimental PzR spectra and the full curves are least-squares fits to a derivative Lorentzian lineshape form of the Aspnes equation [8], which yield parameters of transition energies indicated by arrows. Listed in Table 1 are the values of the excitonic transition energies of $ReS_2$ and $ReSe_2$ at 25 and 300 K. The oscillatory structures on the lower energy side in Fig. 2 are the result of interference effects. There are two dominant features in each of the unpolarized spectra which were related to the band-edge excitonic transitions and were denoted as $E_1^{ex}$ and $E_2^{ex}$ [9]. The in-plane anisotropic effects of the interband transitions near the direct band edge of $ReX_2$ (X=S, Se) indicated that exciton 1 ($E_1^{ex}$) is present only in the $E\|b$ polarization while exciton 2 ($E_2^{ex}$) only appears in the $E\perp b$ polarization. The unpolarized spectra can be regarded as a random superposition of the $E\|b$ and $E\perp b$ polarized spectra. We believe this provides conclusive evidence that both feature 1 and 2 are associated with interband excitonic transitions from different origins.

The absorption-edge anisotropy in $ReS_2$ and $ReSe_2$ single crystals can be studied by measuring the polarization-dependent transmittance spectra. The linearly polarized light used as the probe source was incident normal to the basal plane [$E\|(001)$, $k\perp(001)$]. The absorption coefficient $\alpha$ was determined from the transmittance $T_r$ by taking into account the spectral dependence of the reflectance $R$ using the relation [10]

$$T_r = \frac{(1-R)^2\, e^{-\alpha d}}{1-R^2\, e^{-2\alpha d}} \quad (1)$$

where $d$ is the thickness of the sample.

Eq. (1) assumes that there are multiple reflections within the sample, but that they add incoherently due to sample inhomogeneity or a sufficiently large spread of the incident angles. We also note that the nonuniform thickness and unsmooth sample surface will tend to deviate the incident angles from the normal direction, resulting in some variations in the absorption spectra. Since $\alpha d$ is large for the sample crystals, the second term in the denominator of Eq. (1) can be neglected for the determination of the absorption coefficient $\alpha$.

A more complete analysis, taking into account both the absorption and emission of phonons, is given as follows. For an indirect allowed transition, the absorption coefficient a for a single phonon process can be expressed as [10]

$$\alpha h\nu = \frac{A(h\nu - E_g + E_p)^2}{\exp(E_p/kT)-1} + \frac{B(h\nu - E_g - E_p)^2}{1-\exp(-E_p/kT)} \quad (2)$$

where $h\nu$ is the energy of the incident photon, $E_g$ is the band gap, $E_p$ is the energy of the phonon assisting the transition, and $A$ and $B$ are constants. The first term on the right-hand side of Eq. (2) corresponds to an absorption of a photon and a phonon, whereas the second term corresponds to an absorption of a photon and emission of a phonon and contributes only when $h\nu \geq E_g + E_p$. There is a

Table 1
The energy gaps and excitonic transition energies of $ReX_2$ (X=S, Se) which are derived from the analysis of polarization-dependent absorption and PzR measurements at 25 and 300 K

| Material | $E_{g\|\|}$ (eV) | $E_{g\perp}$ (eV) | $E_p$ (meV) | $E_1^{ex}$ (eV) | $E_2^{ex}$ (eV) | Temperature (K) |
|---|---|---|---|---|---|---|
| $ReS_2$ | 1.51±0.02 | 1.52±0.02 | 22±5 | 1.555±0.002 | 1.587±0.002 | 25 |
| | 1.35±0.02 | 1.38±0.02 | 25±5 | 1.485±0.005 | 1.519±0.005 | 300 |
| $ReSe_2$ | 1.35±0.02 | 1.36±0.02 | 21±5 | 1.387±0.002 | 1.410±0.002 | 25 |
| | 1.18±0.02 | 1.20±0.02 | 25±5 | 1.305±0.005 | 1.323±0.005 | 300 |

large residual absorption at photon energies below the absorption edge. The large values of the absorption coefficient $\alpha$ below the absorption edge of $ReS_2$ and $ReSe_2$ most probably indicate the existence of impurities or defects in the materials. In our present study, the residual absorption is assumed to be a constant and subtracted out for the evaluation of the band gap $E_g$ and phonon energy $E_p$. The data of $ReS_2$ and $ReSe_2$ at 25 and 300 K were then fitted to Eq. (2). Representative results are shown in Fig. 3a and b, where the open circles and solid squares are representative experimental points deduced, respectively from $E\|b$ and $E\perp b$ polarizations transmittance spectra and the solid lines are fitted to Eq. (2). The absorption edge shifted toward higher energies as the temperature of the sample is lowered. The results strongly indicate that $ReS_2$ and $ReSe_2$ are indirect band gap semiconductors, in which $E\|b$ polarization exhibits a smaller band gap and a single phonon makes important contribution in assisting the indirect transitions. Differing values of $E_g$ and $E_p$ could be obtained by fitting a different energy range, for example, by rejecting some points at lower or higher photon energies. From this selective omission of data, an error of the order $\pm 0.02$ eV and $\pm 5$ meV can be deduced for the estimation of $E_g$ and $E_p$, respectively. The fitted values of energy gap and phonon energy of $ReS_2$ are also summarized in Table 1. The value of the phonon energy is $25\pm5$ meV and seems to be insensitive to the temperature. The value of phonon energy shows that it is not an acoustic phonon and very likely originates from one of the numerous optical branches since the optical branches are relatively flat as compared with the acoustic branches. In addition, since the phonon momentum needed for an indirect interband transition is large, agreement of the phonon energies with the zone-center LO phonon energies are not expected. As shown in Table 1, the indirect gaps at 25 and 300 K, denoted as $E_{g\|}$ ($E_{g\perp}$), are respectively determined to be $1.51\pm0.02$ ($1.52\pm0.02$) eV and $1.35\pm0.02$ ($1.38\pm0.02$) eV for $ReS_2$, and $1.35\pm0.02$ ($1.36\pm0.02$) eV and $1.18\pm0.02$ ($1.20\pm0.02$) eV for $ReSe_2$. Here, $E_{g\|}$ and $E_{g\perp}$ refer respectively to the indirect gap of the $E\|b$ and $E\perp b$ polarizations. It is noticed that the value of $E_g$ as determined from the absorption data of the unpolarized incident light lies between $E_{g\|}$ and $E_{g\perp}$. The origin of the unpolarized spectra can be regarded as a random superposition of both the $E\|b$ and $E\perp b$ polarizations spectra. Analysis of the absorption spectra revealed that the values of energy gaps $E_{g\|}$ and $E_{g\perp}$ are slightly different than the previous published works of unpolarized measurements [11,12]. The absorption anisotropy in the van der Waals planes may be a general characteristic of materials with triclinic layered structures.

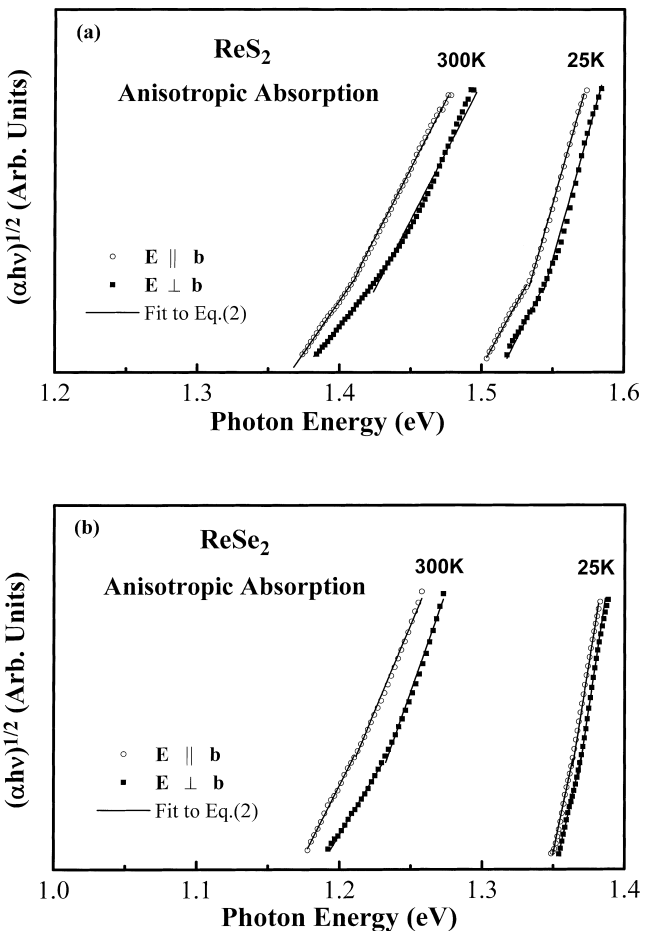


Fig. 3. The experimental points of $(\alpha h\nu)^{1/2}$ vs. $h\nu$ that are deduced from polarization-dependent absorption measurements for (a) $ReS_2$ and (b) $ReSe_2$ at 25 and 300 K, where the open circles (solid squares) are data points from the $E\|b$ ($E\perp b$) polarization measurements and the solid lines are least-squares fits to Eq. (2).

A study of electrical anisotropy of $ReX_2$ along the $b$-axis and perpendicular to the $b$-axis were done by temperature dependent conductivity measurements in the temperature range of 80 to 300 K. For comparison purpose, the conductivity measurement along the $c$ axis was also carried out. Shown in Fig. 4a and b are the temperature dependence of electrical conductivity of $ReS_2$ and $ReSe_2$, where the solid squares, open circles and solid diamonds are data points deduced from the conductivity measurements with the electrical fields along $c$-axis, perpendicular to $b$-axis and parallel to $b$-axis, respectively. The results indicate that $\sigma_{\|b}$ is larger than $\sigma_{\perp b}$ and at least three orders higher than that of $\sigma_{\|c}$ for both $ReS_2$ and $ReSe_2$. The low value of $\sigma_{\|c}$ is a general electrical property of layer-type crystals due to the weak van der Waals bonding between individual layers [1]. The highest value of conductivity parallel to $b$-axis is most likely related to the strongest bonding force of $ReX_2$ which exists along the crystal orientation of Re cluster chains.

## Acknowledgements

The authors C.H. Ho and K.K. Tiong acknowledge the support of the National Science Council of the Republic of

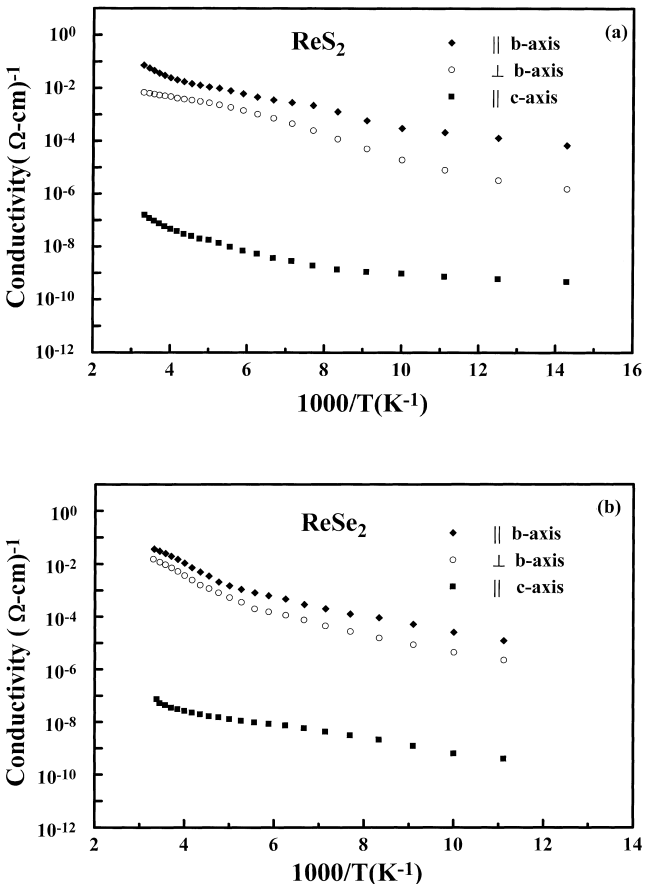


Fig. 4. Temperature dependence of the electrical conductivity of (a) $ReS_2$ and (b) $ReSe_2$. The solid squares, open circles, and solid diamonds are data points deduced from the conductivity measurements with the applied fields along *c*-axis, perpendicular to *b*-axis and parallel to *b*-axis, respectively.

China under Project No. NSC89-2112-M-019-002 and Y.S. Huang acknowledges the support of the National Science Council of the Republic of China under Project No. NSC89-2112-M-011-001.

## References

[1] J.A. Wilson, A.D. Yoffe, Adv. Phys. 18 (1969) 193.
[2] J.C. Wildervanck, F. Jellinek, J. Less-Common Met. 24 (1971) 73.
[3] W.Y. Liang, J. Phys. C: Solid State Phys. 6 (1973) 551.
[4] H.J. Lamfers, A. Meetsma, G.A. Wiegers, J.L. de Boer, J. Alloys Comp. 241 (1996) 34.
[5] C.H. Ho, Y.S. Huang, P.C. Liao, K.K. Tiong, J. Phys. Chem. Solids 60 (1999) 1797.
[6] K. Friemelt, M.-Ch. Lux-Steiner, E. Bucher, J. Appl. Phys. 74 (1993) 5266.
[7] N.W. Alcock, A. Kjekshus, Acta Chem. Scand. 19 (1965) 79.
[8] O.E. Aspnes, in: M. Balkanski) (Ed.), Handbook on Semiconductors, Vol. 2, North Holland, Amsterdam, 1980, p. 109.
[9] C.H. Ho, P.C. Liao, Y.S. Huang, K.K. Tiong, Phys. Rev. B 55 (1997) 25608.
[10] J.I. Pankove, Optical Processes in Semiconductors, Dover, New York, 1975.
[11] J.V. Marzik, R. Kershaw, K. Dwight, A. Wold, J. Solid State Chem. 51 (1984) 170.
[12] C.H. Ho, P.C. Liao, Y.S. Huang, T.R. Yang, K.K. Tiong, J. Appl. Phys. 81 (1997) 6380.